GS2E: Gaussian Splatting is an Effective Data Generator for Event Stream Generation

Yuchen Li[1,*] **Chaoran Feng**[1,*] **Zhenyu Tang**[1] **Kaiyuan Deng**[2] **Wangbo Yu**[1]
Yonghong Tian[1,†] **Li Yuan**[1,†]

[1]Peking University, Shenzhen Graduate School
[2]University of Arizona, Department of Electrical and Computer Engineering
{yuchenli, chaoran.feng, zhenyutang, wbyu}@stu.pku.edu.cn, {yhtian, yuanli-ece}@pku.edu.cn

https://intothemild.github.io/GS2E.github.io/

Figure 1: We propose **GS2E**, a high-fidelity synthetic dataset designed for 3D event-based vision, comprising over **1150** scenes. GS2EExamples of RGB frames and event streams are shown above.

Abstract

We introduce (GS2E) (**G**AUSSIAN **S**PLATTING TO **E**VENT GENERATION), a large-scale synthetic event dataset for high-fidelity event vision tasks, captured from real-world sparse multi-view RGB images. Existing event datasets are often synthesized from dense RGB videos, which typically lack viewpoint diversity and geometric consistency, or depend on expensive, difficult-to-scale hardware setups. GS2E overcomes these limitations by first reconstructing photorealistic static scenes using 3D Gaussian Splatting, and subsequently employing a novel, physically-informed event simulation pipeline. This pipeline generally integrates adaptive trajectory interpolation with physically-consistent event contrast threshold modeling. Such an approach yields temporally dense and geometrically consistent event streams under diverse motion and lighting conditions, while ensuring strong alignment with underlying scene structures. Experimental results on event-based 3D reconstruction demonstrate GS2E's superior generalization capabilities and its practical value as a benchmark for advancing event vision research.

[*]These authors contributed equally to this work.
[†]Corresponding author.

39th Conference on Neural Information Processing Systems (NeurIPS 2025) Track on Datasets and Benchmarks.

1 Introduction

Event cameras, provide high temporal resolution, low latency, and high dynamic range, making them uniquely suited for tasks involving fast motion and challenging lighting conditions [10, 74]. These advantages have been demonstrated in various applications such as autonomous driving [15, 17], drone navigation [56, 5], and 3D scene reconstruction [25, 73, 24, 57, 52, 72]. In particular, their ability to capture asynchronous brightness changes enables accurate motion perception for 3D reconstruction and novel view synthesis (NVS) tasks, surpassing the capabilities of conventional RGB sensors under fast motion and dynamic illumination [75]. However, despite their potential, the advancement of event-based vision algorithms is significantly limited by the scarcity of large-scale, high-quality event datasets, especially those offering multi-view consistency and aligned RGB data. This bottleneck has slowed the development of hybrid approaches that aim to combine event and RGB signals for high-fidelity 3D scene understanding and reconstruction. While event streams provide accurate geometric and motion cues through the high-frequency edge information, RGB frames, often motion-blurred, contribute essential color features with low-frequent details but can suffer from degraded textural information for rendering. While event streams offer precise geometric and motion cues through high-frequency edge information, RGB frames, though often degraded by motion blur, provide complementary low-frequency texture and essential color details for photorealistic rendering. However, the lack of large-scale datasets that jointly exploit these complementary signals limits progress in event-based 3D scene understanding and generation [76]. This aligns with the broader trend of establishing structured evaluation paradigms across domains [34].

As illustrated in Figure 2, existing efforts to conduct event-based 3D reconstruction datasets fall into three main categories: (1) *Real-world capture:* This involves dedicated hardware setups such as synchronized event-RGB stereo rigs or multi-sensor arrays (e.g., DAVIS-based systems [64]). While providing realistic data, these setups are expensive, prone to calibration errors, and difficult to scale to diverse scenes and camera configurations, as seen in systems like Dynamic EventNeRF [58]. (2) *Video-driven synthesis:* v2e [23] and Vid2E [12] generate event streams from dense, high-framerate RGB videos. Although flexible and accessible, they suffer from limited viewpoint diversity and lack geometric consistency, making them suboptimal for multi-view reconstruction tasks. (3) *Simulation via computer graphics engines:* Recent approaches [54, 19, 27, 41] leverage 3D modeling tools like Blender [6] or Unreal Engine [7] to simulate photo-realistic scenes and generate event data along with RGB, depth, and pose annotations. These allow fine-grained control over camera trajectories and lighting, enabling multi-view, physically-consistent dataset synthesis. However, such pipelines may introduce a domain gap due to non-photorealistic rendering or oversimplified dynamics [61].

Video-driven and graphics-based approaches offer greater scalability by enabling controllable and repeatable data generation among above methods. However, video-based methods rely on densely sampled RGB frames from narrow-baseline views, often resulting in motion blur and limited geometric diversity. Simulation with physical engines offers greater control over scenes and trajectories, yet frequently suffer from domain gaps due to non-photorealistic rendering and simplified dynamics [50]. Moreover, an important yet often underexplored factor influencing the realism of synthetic event data is the contrast threshold (CT), which defines the minimum log-intensity change required to trigger an event. While many existing simulators [37, 12] adopt fixed or heuristic CT values, recent analyses [61, 26, 18] show that CT values vary considerably across sensors, scenes, and even within the same sequence. This variability induces a significant distribution shift between synthetic and real event data, thereby limiting the generalization capability of models trained on simulated streams. We posit that accurate modeling of contrast thresholds as data-dependent and adaptive parameters is crucial for generating realistic and transferable event representations. Incorporating physically informed CT sampling, potentially complemented by plausible noise considerations, can significantly enhance sim-to-real transferability in downstream tasks such as 3D reconstruction [79, 9, 78, 9, 86] and optical flow estimation [90, 47, 8, 33, 11].

Based on the above observation, we propose a novel pipeline for synthesizing high-quality, geometry-consistent multi-view event data from sparse RGB inputs. Leveraging 3D Gaussian Splatting (3DGS) [31], we first reconstruct photorealistic 3D scenes from a sparse set of multi-view images with known poses. We then generate continuous trajectories via adaptive interpolation and render dense RGB sequences along these paths. These sequences are fed into our physically-informed event simulator [37]. This simulator employs our data-driven contrast threshold modeling to ensure event responses are consistent with real sensor behaviors, and inherently maintains geometric consistency

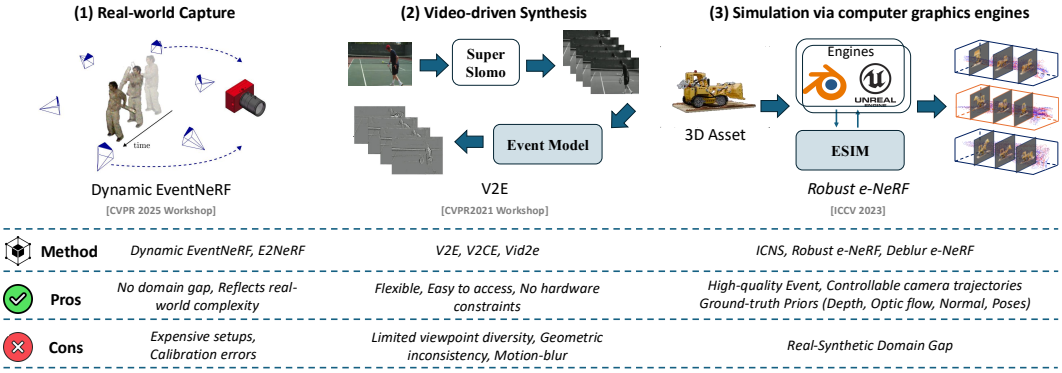

Figure 2: **Overview and comparison of event-based 3D dataset construction methods.** We compare *(1) real-world capture*, *(2) video-driven synthesis*, and *(3) simulation via computer graphics engines* in terms of commonly used methods, strengths, and drawbacks.

through the 3DGS-rendered views and trajectories. Our approach requires no dense input video and preserves the geometric fidelity of the original scene. The controllable virtual setup enables diverse motion patterns and blur levels, supporting the training of robust event-based models.

To summarize, our main contributions are:

- We propose a novel simulation pipeline for generating multi-view event data from sparse RGB images, leveraging 3DGS for high-fidelity reconstruction and novel view synthesis.
- We propose an adaptive trajectory interpolation strategy coupled with a physically-grounded contrast threshold model, jointly enabling the synthesis of temporally coherent and sensor-consistent event streams.
- We construct and release a benchmark dataset comprising photorealistic RGB frames, motion-blurred sequences, accurate camera poses, and multi-view event streams, facilitating research in structure-aware event vision.

2 Related Work

2.1 Optimization-based Event Simulators

Early event simulation methods, such as those proposed by Kaiser et al.[29] and Mueggler et al.[45], generated events by thresholding frame differences or rendering high-framerate videos. However, these approaches failed to capture the inherent asynchronous and low-latency characteristics of event sensors. Subsequent works like ESIM [54] and Vid2E [13] improved realism by incorporating per-pixel log-intensity integration and optical flow-based interpolation to approximate event triggering more faithfully. V2E [23] further advanced realism by modeling sensor-level attributes such as bandwidth limitations, background activity noise, and Poisson-distributed firing. More recent simulators including V2CE [84], ICNS [28], and DVS-Voltmeter [37], introduced hardware-aware components, accounting for effects such as latency, temperature-dependent noise, and local motion dynamics. PECS [20] extended this direction by modeling the full optical path through multispectral photon rendering. Despite their increased physical fidelity, most of these simulators operate purely on 2D image or video inputs and do not exploit the underlying 3D structure of scenes. Furthermore, the prevalent use of fixed contrast thresholds across all viewpoints and scenes fails to reflect the variability observed in real sensors, thereby introducing a significant domain gap in simulated data.

2.2 Learning-based Event Simulators

Recent efforts have explored deep learning to synthesize event streams in a data-driven manner. EventGAN [89] employed GANs to generate event frames from static images, while Pantho et al. [48] learned to generate temporally consistent event tensors or voxel representations. Domain-adaptive simulators such as Gu et al. [16] jointly synthesized camera trajectories and event data, improving realism under target distributions. However, learning-based approaches generally suffer

from limited interpretability and require retraining when transferred to new scenarios, leading to weaker robustness compared to physics-inspired models. In contrast, our method follows a physically grounded yet geometry-aware paradigm: we first reconstruct high-fidelity 3D scenes via 3DGS then synthesize event streams by simulating photorealistic motion blur and modeling the contrast threshold distribution observed in real-world data. This enables us to generate temporally coherent, multi-view consistent event data with improved realism and transferability.

3 Method

3.1 Preliminary

3D Gaussian Splatting. 3D Gaussian Splatting [31] represents a scene as a set of anisotropic Gaussians. Each Gaussian G_i is defined by

$$G_i(\mathbf{x}) = \exp\Big(-\tfrac{1}{2}\,(\mathbf{x}-\boldsymbol{\mu}_i)^\top(\mathbf{R}_i\,\mathrm{diag}(\mathbf{s}_i)^2\,\mathbf{R}_i^\top)^{-1}(\mathbf{x}-\boldsymbol{\mu}_i)\Big), \tag{1}$$

where $\boldsymbol{\mu}_i \in \mathbb{R}^3$ is the mean, $\mathbf{q}_i \mapsto \mathbf{R}_i \in \mathrm{SO}(3)$ is the rotation, and $\mathbf{s}_i \in \mathbb{R}^3_+$ is the scale. View-dependent radiance coefficients $\mathbf{c}_i$ and opacity $\alpha_i \in [0,1]$ are optimized via differentiable rasterization under an ℓ_1 photometric loss. Each Gaussian is transformed by the camera pose $\mathbf{T} \in \mathrm{SE}(3)$ and projected at render time, then the resulting 2D covariance is

$$\boldsymbol{\Sigma}_i' = \mathbf{J}_i\,\mathbf{T}\,\boldsymbol{\Sigma}_i\,\mathbf{T}^\top\,\mathbf{J}_i^\top, \tag{2}$$

where $\mathbf{J}_i$ denotes the Jacobian of the projection and each pixel colors $\hat{C}$ are composited as follows:

$$\hat{C} = \sum_{k\in\mathcal{N}} \mathbf{c}_k\,\alpha_k \prod_{j<k}(1-\alpha_j). \tag{3}$$

Event Generation Model. Event cameras produce an asynchronous stream of tuples (x, y, t_i, p_i) by thresholding changes in log-irradiance [10, 14]. Denoting the last event time at pixel (x, y) by t_{ref}, define as:

$$\Delta \log L = \log L_{(x,y)}(t_i) - \log L_{(x,y)}(t_{\mathrm{ref}}). \tag{4}$$

An event of polarity $p_i \in \{+1, -1\}$ is emitted whenever $|\Delta \log L| \geq c$:

$$p_i = \begin{cases} +1, & \Delta \log L \geq c, \\ -1, & \Delta \log L \leq -c. \end{cases} \tag{5}$$

After each event, t_{ref} is updated to t_i. This simple thresholding mechanism yields a high-temporal-resolution, sparse stream of brightness changes suitable for downstream vision tasks. Here, we introduce the off-the-shell model DVS-Voltmeter [37] as the event generation model, which incorporates physical characteristics of DVS circuits. Unlike deterministic models, DVS-Voltmeter treats the voltage evolution at each pixel as a stochastic process, specifically a Brownian motion with drift. In this formulation, the photovoltage change ΔV_d over time is modeled as

$$\Delta V_d(t) = \mu \Delta t + \sigma W(\Delta t), \tag{6}$$

where μ is a drift term capturing systematic brightness changes, σ denotes the noise scale influenced by photon reception and leakage currents, and $W(\cdot)$ represents a standard Brownian motion. Events are then generated when the stochastic voltage process crosses either the *ON* or *OFF* thresholds. This physics-inspired modeling enables it to produce events with realistic timestamp randomness and noise characteristics, providing more faithful supervision for event-based vision tasks.

3.2 Pipeline Overview

Our pipeline generates multi-view, geometry-consistent event data from sparse RGB inputs. The process begins with collecting sparse multi-view RGB images along with their corresponding camera poses (§3.3). Using these inputs, we reconstruct high-fidelity scene geometry and appearance via 3DGS [31] (§3.4), providing a solid foundation for the subsequent steps. To simulate diverse observations, we generate smooth, controllable virtual camera trajectories by reparameterizing the original pose sequence based on velocity constraints, followed by interpolation of dense viewpoints along the trajectory (§3.5). Finally, the generated RGB sequences are fed into our optimized event generation module to synthesize temporally coherent, multi-view-consistent event streams (§3.7). This well-structured pipeline enables scalable and controllable event data generation from sparse RGB inputs, ensuring both accuracy and efficiency. The overall pipeline is shown in Figure 3.

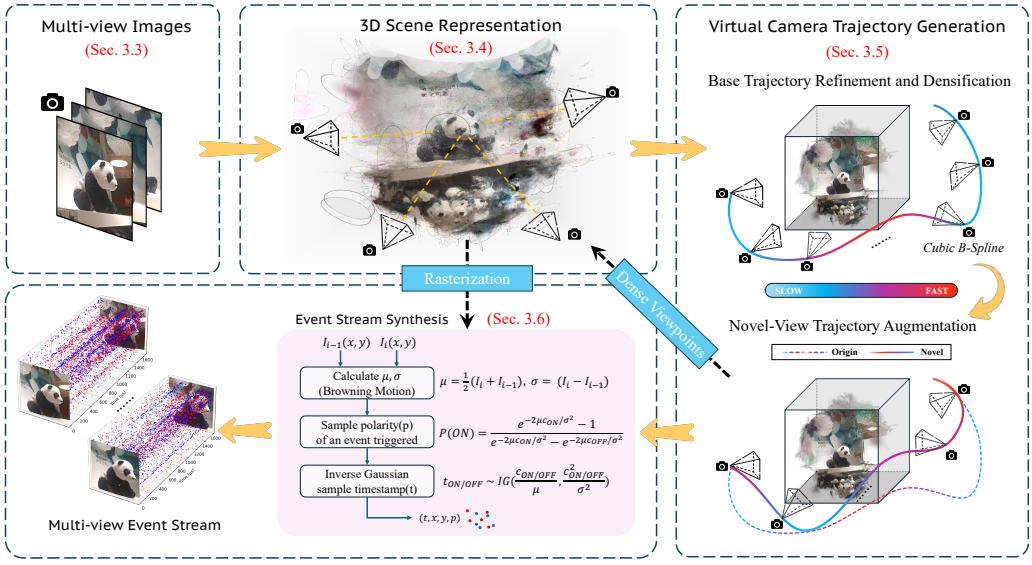

Figure 3: Overview of the proposed **GS2E** pipeline. Starting from sparse multi-view RGB images and known camera poses, we reconstruct high-fidelity scene representations using 3D Gaussian Splatting. Virtual camera trajectories are then synthesized via velocity-aware reparameterization and interpolation. The rendered image sequences are passed to a volumetric event simulator to generate temporally coherent and geometrically consistent event streams.

3.3 Data Collection

To support high-fidelity reconstruction and geometry-consistent event generation, we leverage two complementary datasets. The first is MVImgNet [80], a large-scale multi-view image collection comprising 6.5 million frames from 219,199 videos across 238 object categories. We sample **1,000** diverse scenes suitable for 3D reconstruction and motion-aware event synthesis from this dataset. To supplement MVImgNet's object-centric diversity with scene-level structural richness, we incorporate DL3DV [38], a dense multi-view video dataset offering accurate camera poses and ground-truth depth maps across 10,000 photorealistic indoor and ourdoor scenes. We also sample **50** diverse scenes from its 140 benchmark scenes. DL3DV provides high-quality geometry and illumination cues that are critical for evaluating spatial and temporal consistency in event simulation.

Totally, we select **1050** scenes from these datasets which enable us to construct a diverse benchmark for sparse-to-event generation, supporting both object-level and scene-level evaluation under motion blur and asynchronous observation conditions.

3.4 3D Scene Representation

We employ 3DGS as detailed in §3.1 to reconstruct high-fidelity 3D scenes from sparse input views. These views are represented by their corresponding camera poses $\{P_i = (R_i, \mathbf{T}_i)\}_{i=1}^{N}$, where $R_i \in \mathrm{SO}(3)$ is the rotation matrix, and $\mathbf{T}_i \in \mathbb{R}^3$ is the translation vector. For the MVImgnet and DL3DV datasets, we typically use $N = 30$ and 100 for the number of input views. Given the image sequence $\{I_i\}_{i=1}^{N}$, we train a 3DGS model for 30,000 iterations to reconstruct a high-fidelity 3D radiance field. This radiance field captures both the scene's geometry and appearance, serving as the foundation for subsequent trajectory interpolation and event stream synthesis.

3.5 Virtual Camera Trajectory Generation

To simulate continuous camera motion essential for realistic event data synthesis, we transform the initial discrete set of camera poses, often obtained from structure-from-motion with COLMAP [59], into temporally dense and spatially smooth trajectories. This process involves two primary stages: (1) initial trajectory refinement and adaptive densification, (2) followed by an optional augmentation stage for enhanced motion diversity.

3.5.1 Base Trajectory Refinement and Densification

The raw camera poses $\{P_i = (R_i, \mathbf{T}_i)\}_{i=1}^{N}$ can exhibit jitter or abrupt transitions, detrimental to high-fidelity event simulation. We first address this through local pose smoothing and then generate a dense base trajectory using velocity-controlled interpolation.

Pose Stabilization via Local Trajectory Smoothing. To mitigate local jitter and discontinuities, we apply a temporal smoothing filter to the original camera poses. For each pose P_i, we define a local temporal window $\mathcal{W}_i = \{P_j \mid |j - i| \leq w,\ j \in N^+\}$ with a half-width w (e.g., $w = 2$). The smoothed pose $P_i' = (R_i', \mathbf{T}_i')$ is computed as:

$$\mathbf{T}_i' = \frac{1}{|\mathcal{W}_i|} \sum_{j \in \mathcal{W}_i} \mathbf{T}_j, \tag{7}$$

$$R_i' = \mathrm{Slerp}\left(\{R_j\}_{j \in \mathcal{W}_i}, \frac{1}{2}\right), \tag{8}$$

where $\mathrm{Slerp}(\cdot)$ denotes spherical linear interpolation of rotations, evaluated at the temporal midpoint of the window. This procedure enhances local continuity, yielding a smoothed sequence $\{P_i'\}_{i=1}^{N}$ suitable for subsequent densification.

Velocity-Controlled Dense Interpolation. Building upon the smoothed poses $\{P_i'\}$, we generate a temporally uniform but spatially adaptive dense trajectory. Given a desired interpolation multiplier $\gamma > 1$, the target number of poses in the dense trajectory is $M = \lceil \gamma \cdot N \rceil$. These poses, $\{\tilde{P}_j = (\tilde{R}_j, \tilde{\mathbf{T}}_j)\}_{j=0}^{M-1}$, are sampled at evenly spaced normalized time steps $t_j = j/(M-1)$. To achieve adaptive spatial sampling, we first quantify the motion between adjacent smoothed poses. The displacement δ_i between P_i' and P_{i+1}' is defined as a weighted combination of rotational and translational changes:

$$\delta_i = \alpha \cdot \theta_i + \beta \cdot \|\mathbf{T}_{i+1}' - \mathbf{T}_i'\|_2, \tag{9}$$

where $\theta_i = \cos^{-1}\left(\frac{\mathrm{Tr}(R_{i+1}'(R_i')^\top) - 1}{2}\right)$ is the geodesic distance between orientations R_i' and R_{i+1}', and α, β are weighting coefficients. The cumulative path length up to pose P_i' is $s_i = \sum_{k=0}^{i-1} \delta_k$, with $s_0 = 0$. The total path length is s_{N-1}. We then introduce a user-defined velocity profile, which can be a continuous function $v(t)$ or a discrete list $\{v_k\}_{k=0}^{M-2}$, controlling the desired speed along the trajectory. This profile dictates the sampling density: higher velocities lead to sparser sampling in terms of path length per time step. The target path length $\tilde{s}_j$ corresponding to each time step t_j is computed by normalized cumulative velocity:

$$\tilde{s}_j = s_{N-1} \cdot \frac{\sum_{k=0}^{j-1} v_k \cdot \Delta t}{\sum_{l=0}^{M-2} v_l \cdot \Delta t}, \tag{10}$$

where $\Delta t = 1/(M-1)$. Finally, we fit a cubic B-spline curve to the control points $\{(s_i, P_i')\}$ (parameterized by cumulative path length s_i) and sample this spline at the reparameterized path lengths $\{\tilde{s}_j\}$ to obtain the dense trajectory $\{\tilde{P}_j\}$. This base trajectory serves as a foundation for rendering image sequences.

3.5.2 Novel-View Trajectory Augmentation for Enhanced Motion Diversity

To further enrich the dataset with varied camera movements, we generate multiple *novel-view mini-trajectories*. These are derived by sampling keyframes from the dense base trajectory $\{\tilde{P}_j\}_{j=0}^{M-1}$ (generated in §3.5.1) and interpolating new paths between them. Specifically, we uniformly sample G groups of K keyframes from $\{\tilde{P}_j\}$ without replacement:

$$\mathcal{K}_g = \left\{\tilde{P}_{i_1}^{(g)}, \ldots, \tilde{P}_{i_K}^{(g)}\right\} \subset \{\tilde{P}_j\}, \quad g = 1, \ldots, G, \tag{11}$$

where $K \leq K_{\max}$ is the number of keyframes per mini-trajectory and we set $K = 5$. For each group $\mathcal{K}_g$, we compute cumulative pose displacements along its K keyframes using the metric δ_k (Eq. 9), resulting in a local path length s'_{K-1}. We then generate F uniformly spaced spatial targets along this local path:

$$\hat{s}_\ell = \frac{\ell \cdot s'_{K-1}}{F - 1}, \quad \ell = 0, \ldots, F-1. \tag{12}$$

Novel-view poses $\{\hat{P}_\ell^{(g)}\}_{\ell=0}^{F-1}$ are interpolated by fitting either a cubic B-spline or a Bézier curve (with a randomly selected degree $d \in \{2, 3, 4, 5\}$) to the keyframes in $\mathcal{K}_g$, parameterized by their local cumulative path length, and then sampling at $\{\hat{s}_\ell\}$. Each interpolated pose $\hat{P}_\ell^{(g)}$ inherits its camera intrinsics from the first keyframe $\tilde{P}_{i_1}^{(g)}$ in its group. Each resulting sequence $\mathcal{C}_g = \{\hat{P}_\ell^{(g)}\}_{\ell=0}^{F-1}$ constitutes a geometry-consistent, temporally uniform mini-trajectory. The collection of all G groups, $\{\mathcal{C}_g\}_{g=1}^{G}$, provides a diverse set of camera motions. In our experiments, we typically set $G = 3$ and $F = 150$. These augmented trajectories, along with the base trajectory, are used for rendering image sequences for event synthesis.

3.6 Optimize Novel View Synthesis of RGB Domain

Event synthesis is highly sensitive to minute radiometric variations and sensor noise; hence the fidelity of RGB novel view synthesis (NVS) that drives simulation is critical. Because 3DGS is a lossy reconstruction, naïve renderings may contain subtle artifacts (e.g., incompletely reconstructed fine textures) that are amplified in the event domain. We therefore explicitly optimize the RGB NVS stage.

We adopt three complementary measures to improve RGB view fidelity before event simulation: (i) *Data curation.* We use densely covered multi-view datasets (DL3DV, MVImgNet) and apply manual screening plus task-driven filtering; scenes with poor downstream performance (event-based 3D reconstruction, video reconstruction, deblurring) are removed. (ii) *RGB NVS enhancement.* A diffusion-based RGB refinement module, Difix3D+ [71], is applied on top of 3DGS to suppress holes/artifacts while preserving geometry, recovering rich textures and crisp edges without altering camera parameters. (iii) *Decoupled event noise.* RGB denoising is kept separate from event-domain stochasticity: the physically informed simulator governs event noise via sensor models like threshold distribution, preventing uncontrolled propagation of RGB artifacts.

The improvement achieved by incorporating this module is evident, with specific results detailed in the quantitative analysis of the experimental section.(§4.4)

3.7 Event Synthesis from Rendered Sequences

Given high-temporal-resolution image sequences rendered along diverse virtual camera trajectories (§3.5), we synthesize event streams using the DVS-Voltmeter model [37], which stochastically models pixel-level voltage accumulation. This simulator provides temporally continuous and probabilistically grounded event generation, effectively mitigating aliasing artifacts introduced by 3DGS rasterization [31], especially under fast camera motion.

As discussed in Eq. (5) (§3.1), a key parameter is the *contrast threshold* c, denoting the minimum log-intensity change required to trigger an event. Following the calibration strategy of Stoffregen et al. [61], we empirically sweep c within $[0.25, 1.5]$, observing that:

- Low thresholds ($c \leq 0.4$) yield dense, low-noise events, resembling IJRR [46], but may introduce *floater artifacts* when used with 3DGS (see §B).
- High thresholds ($c \geq 0.8$) produce sparse events with pronounced dynamic features, similar to MVSEC [88].

The target datasets, MVImgNet [80] and DL3DV [38], generally exhibit moderate motion and textured surfaces, statistically between IJRR and HQF [61]. Based on this observation and experimental validation (§4), we adopt $c \in [0.2, 0.5]$, balancing fine detail preservation and temporal coherence through the stochastic nature of the Voltmeter model.

4 Experiments

Implementation details. For the reconstruction stage, we carefully collect approximately 2k high-quality multi-view images from 2 public datasets: MVImageNet [80] and DL3DV [38]: we choose and render 1.8k scenes from MVImageNet and 100 scenes from DL3DV. We employ the official interplementation verision of 3DGS [31] in the original setting. For the event generation stage, we utilize the DVS-Voltmeter simulator [37] to synthesize events from the rendered RGB sequences. We

adopt the following sensor-specific parameters to closely mimic the behavior of real DVS sensors: the ON and OFF contrast thresholds are both set to $\Theta_{ON} = \Theta_{OFF} = 1$ as default. We conduct our experiment on the NVIDIA RTX 3090 24GB, and more details and settings are in the appendix.

Evaluation Baselines and Metrics. We evaluate the proposed dataset across three key dimensions: (1) 3D reconstruction quality (§4.1), (2) the domain gap between synthetic and real-world event streams (§4.2), and (3) applicability to a range of downstream tasks (§4.3). For reconstruction-related evaluations, we adopt standard full-reference image quality metrics: PSNR, SSIM [70], and LPIPS [83], to assess both novel view synthesis and event-based deblurring performance. To further evaluate perceptual quality in image restoration and video interpolation tasks, we also employ no-reference metrics, including CLIPIQA [67], MUSIQ [30], and RANKIQA [40]. These metrics help quantify the realism, fidelity, and temporal consistency of outputs under different usage scenarios.

4.1 Reliability of 3D Reconstruction

We trained the 3DGS model on the MVImgNet dataset following a rigorous selection of input views and optimized the model for 30,000 iterations. We then evaluated its rendering fidelity against the ground-truth test set. Quantitative results demonstrate high reconstruction quality, with an average PSNR of 29.8, SSIM of 0.92, and a perceptual LPIPS score of 0.14. These results establish a solid foundation for leveraging 3DGS as a core module for camera pose control, high frame-rate interpolation, and photorealistic rendering, thereby enabling physically grounded event simulation.

4.2 Reliability of event sequences

Due to the lack of widely accepted quantitative metrics for evaluating event data quality, recent proposals such as the Event Quality Score (EQS) [3] offer promising directions for future research. However, as the EQS implementation is not publicly available.

Therefore, we first performed qualitative evaluations using real-world RGB-event datasets. Specifically, we employed the DSEC dataset from the Robotics and Perception Group at the University of Zurich, which provides synchronized recordings from RGB and DVS cameras in driving scenarios. To approximate static 3D scene conditions, we selected scenes with rigid object motion and limited amplitude variation. Visual comparisons demonstrate that our method produces event distributions more consistent with real data than conventional video-driven synthesis approaches.

Afterward, to objectively assess event-stream fidelity, we carefully reproduce the EQS on *10 real scenes* from the DSEC dataset, where ground-truth events are available. We compare video-to-event methods (Vid2e, v2e) with our GS2E, and an enhanced variant with Difix3D+.

Table 1: Evaluation of the event stream quality with the DSEC dataset (↑: higher is better).

Metric	Vid2e	v2e	GS2E	GS2E+Difix3D+
EQS↑	0.725	0.738	**0.761**	**0.782**

GS2E achieves higher EQS than Vid2e and v2e, and further improves with Difix3D+. We attribute these gains to: (i) scene-consistent multi-view synthesis that enables dense, artifact-reduced event generation across views; and (ii) physically informed noise modeling that captures realistic sensor behaviors without temporal jitter or stereo mismatch typical of real sensors.

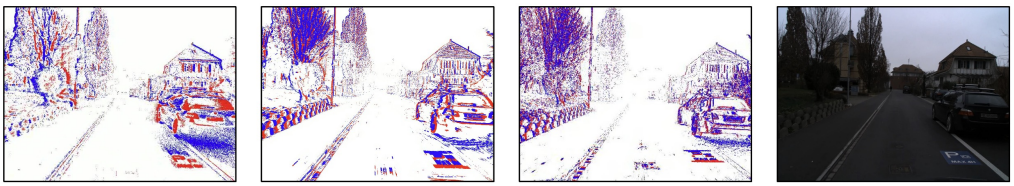

V2E GS2E (Ours) GT Event GT RGB

Figure 4: Qualitative comparison of synthesized event distributions using GS2E versus traditional video-driven event synthesis methods, evaluated against real-world event data from the DSEC dataset.

(a) Event-vision Task: 3D Reconstruction (b) Event-vision Task: Image Deblurring

Figure 5: Application to Multiple Tasks. We benchmark it across event-vision tasks: 3D reconstruction and image deblurring.

Table 2: Comparison of different methods under varying motion speeds. Metrics are averaged over each category (↑: higher is better; ↓: lower is better).

Category	Method	*Mild Speed*			*Medium Speed*			*Strong Speed*		
		PSNR↑	SSIM↑	LPIPS↓	PSNR↑	SSIM↑	LPIPS↓	PSNR↑	SSIM↑	LPIPS↓
Event-only	E-NeRF [32]	21.67	0.827	0.216	20.93	0.815	0.244	20.11	0.792	0.260
	Event-3DGS [18]	11.19	0.623	0.649	10.34	0.387	0.695	10.68	0.374	0.712
Event-fusion	E-NeRF [32]	21.89	0.834	0.208	21.05	0.820	0.239	20.57	0.809	0.251
	Event-3DGS [18]	24.31	0.884	0.118	21.88	0.832	0.224	19.36	0.793	0.295

4.3 Application to Multiple Tasks

To evaluate the generalization and practicality of our proposed event dataset, we benchmark it across three event-vision tasks: 3D reconstruction, image deblurring, and image/video reconstruction. For all tasks, we compare several state-of-the-art methods, and report standard image quality metrics.

Event-based 3D Reconstruction. We first evaluate the utility of our dataset in static 3D scene reconstruction. To assess robustness under motion-induced challenges, we simulate static scenes with varying camera motion speeds (*mild, medium*, and *strong*), allowing controlled evaluation of temporal consistency and appearance fidelity. We further compare grayscale-only and RGB-colored supervision settings to investigate the effect of color information. As shown in Table 2, while all methods exhibit performance drops under faster motion, models trained with color supervision consistently achieve better perceptual quality. These results highlight the versatility of our dataset in supporting both grayscale and color-aware pipelines, and its suitability for evaluating spatiotemporal consistency in static scenes captured via asynchronous event observations.

Event-based Image Deblurring. We further test whether event streams generated from our dataset can support high-quality image restoration under motion blur. Leveraging recent event-guided deblurring frameworks [60, 62], we evaluate reconstruction performance using both synthetic blurry frames paired with our event data. The results indicate that our dataset effectively captures motion-dependent blur patterns and high-frequency temporal cues, which help deblurring models produce sharper and more temporally consistent outputs, particularly in low-light and fast-moving scenes.

Table 3: Comparison of image deblurring and video reconstruction methods.

Method	**PSNR↑**	**SSIM↑**	**LPIPS↓**
Deblurring Task			
D2Net [60]	29.61	0.932	0.113
EFNet [62]	31.26	0.940	0.098

Method	**CLIPIQA↑**	**MUSIQ↑**	**RANKIQA↓**
Video Reconstruction Task			
E2VID [55]	0.139	46.52	4.879
TimeLen++ [65]	0.144	48.68	4.325

Event-based Video Reconstruction. Finally, we assess the utility of GS2E as a benchmark for event-driven video reconstruction tasks [55, 65], including frame interpolation and intensity reconstruction. Owing to its fine-grained temporal resolution, accurate camera motion, and realistic lighting variations, GS2E provides a challenging yet structured testbed for evaluating reconstruction quality under high-speed motion. As shown in Table 3, existing models exhibit improved motion continuity and reduced ghosting artifacts when evaluated on our dataset, highlighting its effectiveness.

Table 4: RGB NVS quality before event simulation. Higher is better for PSNR/SSIM; lower is better for LPIPS.

	PSNR ↑		SSIM ↑		LPIPS ↓	
Scene	3DGS	+Difix3D+	3DGS	+Difix3D+	3DGS	+Difix3D+
Scene_1	29.10	31.64	0.945	0.953	0.171	0.162
Scene_2	32.01	33.82	0.939	0.951	0.117	0.109
Scene_3	28.98	30.15	0.936	0.944	0.143	0.131
Scene_4	38.41	38.63	0.959	0.960	0.158	0.159
Scene_5	35.79	36.29	0.967	0.969	0.071	0.064
Scene_6	31.81	33.32	0.934	0.947	0.318	0.292
Scene_7	29.26	32.49	0.942	0.968	0.151	0.137
Scene_8	32.88	34.21	0.928	0.941	0.153	0.126
Scene_9	30.87	31.95	0.928	0.940	0.240	0.228
Scene_10	30.67	32.48	0.895	0.914	0.290	0.291
Scene_11	35.29	36.03	0.955	0.956	0.261	0.260
Average	**32.28**	**33.73**	**0.939**	**0.949**	**0.188**	**0.178**

4.4 Ablation study

Interplation Methods of Trajectory. To analyze how different interpolation strategies influence the quality of synthesized event streams and their impact on downstream reconstruction tasks, we compare linear, Bézier, and cubic B-spline methods for virtual camera trajectory generation, shown as in Figure 6. While linear interpolation is efficient, its velocity discontinuities at control points can undermine temporal coherence in high-fidelity reconstruction. Cubic B-splines, by ensuring smooth higher-order continuity, yield more realistic trajectories. We thus use cubic B-spline interpolation with velocity control as the default, balancing smoothness and trajectory realism.

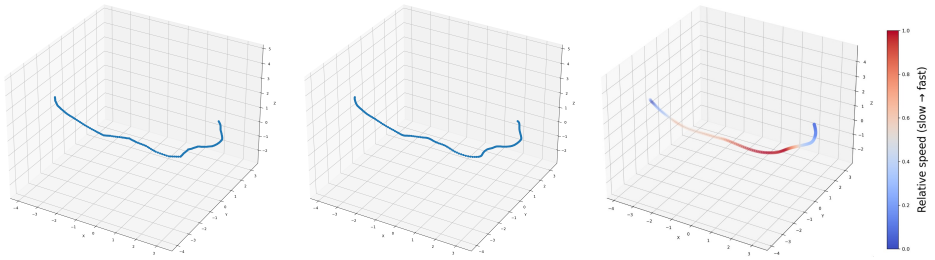

Linear Interpolation | Bézier Interpolation | Velocity-Controlled Dense B-spline Interpolation (Ours)

Figure 6: Comparison of different interpolation methods shows that our method is smoother and has speed control capabilities.

The Generative Refinement Module We evaluate the effect of the RGB enhancement on static scenes from DL3DV and MVImgNet using PSNR, SSIM, and LPIPS. Table 4 reports per-scene results for 3DGS and 3DGS&Difix3D+[71]. The enhancement yields consistent gains across 11 scenes: average *PSNR* increases by **+1.45 dB** (min +0.22 dB, max +3.23 dB), *SSIM* improves by **+0.010**, and *LPIPS* decreases by **0.010** on average. These results indicate that RGB novel views entering the event simulator are of sufficiently high fidelity and reduced artifact levels, addressing the risk of artifact-induced spurious events.

5 Conclusion

We introduced GS2E, a large-scale dataset that synthesizes high-fidelity event streams from sparse multi-view RGB. Our pipeline couples 3DGS reconstruction with a physically grounded simulator, featuring adaptive trajectory interpolation and contrast-threshold modeling, and employs a diffusion-based RGB refinement module to reduce artifacts before event simulation. This yields temporally dense, geometry-consistent events under diverse motion and lighting. Experiments show clear gains on downstream tasks (e.g., event-based 3D reconstruction and video interpolation). Future work will incorporate exposure-aware camera models into 3DGS and extend to dynamic scenes.

Acknowledgment

This work was supported in part by the Natural Science Foundation of China (No. 62332002, 62202014, 62425101)

References

[1] Anish Bhattacharya, Ratnesh Madaan, Fernando Cladera, Sai Vemprala, Rogerio Bonatti, Kostas Daniilidis, Ashish Kapoor, Vijay Kumar, Nikolai Matni, and Jayesh K Gupta. Evdnerf: Reconstructing event data with dynamic neural radiance fields. In *Proceedings of the IEEE/CVF Winter Conference on Applications of Computer Vision*, pages 5846–5855, 2024.

[2] Marco Cannici and Davide Scaramuzza. Mitigating motion blur in neural radiance fields with events and frames. In *Proceedings of the IEEE/CVF Conference on Computer Vision and Pattern Recognition (CVPR)*, 2024.

[3] Kaustav Chanda, Aayush Atul Verma, Arpitsinh Vaghela, Yezhou Yang, and Bharatesh Chakravarthi. Event quality score (eqs): Assessing the realism of simulated event camera streams via distances in latent space, 2025.

[4] Kang Chen, Jiyuan Zhang, Zecheng Hao, Yajing Zheng, Tiejun Huang, and Zhaofei Yu. Uspgaussian: Unifying spike-based image reconstruction, pose correction and gaussian splatting. *arXiv preprint arXiv:2411.10504*, 2024.

[5] Peiyu Chen, Weipeng Guan, and Peng Lu. Esvio: Event-based stereo visual inertial odometry. *IEEE Robotics and Automation Letters*, 8(6):3661–3668, 2023.

[6] Blender Online Community. *Blender - a 3D modelling and rendering package*. Blender Foundation, Stichting Blender Foundation, Amsterdam, 2018.

[7] Unreal Engine. Unreal engine. *Retrieved from Unreal Engine: https://www. unrealengine. com/en-US/what-is-unreal-engine-4*, 2018.

[8] Zhenxuan Fang, Fangfang Wu, Weisheng Dong, Xin Li, Jinjian Wu, and Guangming Shi. Self-supervised non-uniform kernel estimation with flow-based motion prior for blind image deblurring. In *Proceedings of the IEEE/CVF Conference on Computer Vision and Pattern Recognition*, pages 18105–18114, 2023.

[9] Chaoran Feng, Wangbo Yu, Xinhua Cheng, Zhenyu Tang, Junwu Zhang, Li Yuan, and Yonghong Tian. Ae-nerf: Augmenting event-based neural radiance fields for non-ideal conditions and larger scene. *arXiv preprint arXiv:2501.02807*, 2025.

[10] Guillermo Gallego, Tobi Delbrück, Garrick Orchard, Chiara Bartolozzi, Brian Taba, Andrea Censi, Stefan Leutenegger, Andrew J Davison, Jörg Conradt, Kostas Daniilidis, et al. Event-based vision: A survey. *IEEE Trans. Pattern Analysis and Machine Intelligence (PAMI)*, 2020.

[11] Guillermo Gallego, Henri Rebecq, and Davide Scaramuzza. A unifying contrast maximization framework for event cameras, with applications to motion, depth, and optical flow estimation. In *Proceedings of the IEEE conference on computer vision and pattern recognition*, pages 3867–3876, 2018.

[12] Daniel Gehrig, Mathias Gehrig, Javier Hidalgo-Carrió, and Davide Scaramuzza. Video to events: Recycling video datasets for event cameras. In *Computer Vision and Pattern Recognition (CVPR)*, 2020.

[13] Daniel Gehrig, Mathias Gehrig, Javier Hidalgo-Carrió, and Davide Scaramuzza. Video to events: Recycling video datasets for event cameras. In *Proceedings of the IEEE/CVF Conference on Computer Vision and Pattern Recognition*, pages 3586–3595, 2020.

[14] Daniel Gehrig, Antonio Loquercio, Konstantinos G Derpanis, and Davide Scaramuzza. End-to-end learning of representations for asynchronous event-based data. In *Proceedings of the IEEE/CVF International Conference on Computer Vision*, pages 5633–5643, 2019.

[15] Mathias Gehrig, Willem Aarents, Daniel Gehrig, and Davide Scaramuzza. DSEC: A stereo event camera dataset for driving scenarios. *IEEE Robotics and Automation Letters*, 2021.

[16] Daxin Gu, Jia Li, Yu Zhang, and Yonghong Tian. How to learn a domain-adaptive event simulator? In *Proceedings of the 29th ACM International Conference on Multimedia*, pages 1275–1283, 2021.

[17] Shuang Guo and Guillermo Gallego. Cmax-slam: Event-based rotational-motion bundle adjustment and slam system using contrast maximization. *IEEE Transactions on Robotics*, 2024.

[18] Haiqian Han, Jianing Li, Henglu Wei, and Xiangyang Ji. Event-3dgs: Event-based 3d reconstruction using 3d gaussian splatting. *Advances in Neural Information Processing Systems*, 37:128139–128159, 2024.

[19] Haiqian Han, Jiacheng Lyu, Jianing Li, Henglu Wei, Cheng Li, Yajing Wei, Shu Chen, and Xiangyang Ji. Physical-based event camera simulator. In *European Conference on Computer Vision*, pages 19–35. Springer, 2024.

[20] Haiqian Han, Jiacheng Lyu, Jianing Li, Henglu Wei, Cheng Li, Yajing Wei, Shu Chen, and Xiangyang Ji. Physical-based event camera simulator. In *Computer Vision – ECCV 2024: 18th European Conference, Milan, Italy, September 29–October 4, 2024, Proceedings, Part XLV*, page 19–35, Berlin, Heidelberg, 2024. Springer-Verlag.

[21] Weihua He, Kaichao You, Zhendong Qiao, Xu Jia, Ziyang Zhang, Wenhui Wang, Huchuan Lu, Yaoyuan Wang, and Jianxing Liao. Timereplayer: Unlocking the potential of event cameras for video interpolation. In *Proceedings of the IEEE/CVF Conference on Computer Vision and Pattern Recognition*, pages 17804–17813, 2022.

[22] Javier Hidalgo-Carrió, Guillermo Gallego, and Davide Scaramuzza. Event-aided direct sparse odometry. In *Proceedings of the IEEE/CVF Conference on Computer Vision and Pattern Recognition*, pages 5781–5790, 2022.

[23] Yuhuang Hu, Shih-Chii Liu, and Tobi Delbruck. v2e: From video frames to realistic dvs events. In *Proceedings of the IEEE/CVF Conference on Computer Vision and Pattern Recognition*, pages 1312–1321, 2021.

[24] Jian Huang, Chengrui Dong, and Peidong Liu. Inceventgs: Pose-free gaussian splatting from a single event camera. *arXiv preprint arXiv:2410.08107*, 2024.

[25] Inwoo Hwang, Junho Kim, and Young Min Kim. Ev-nerf: Event based neural radiance field. In *Proceedings of the IEEE/CVF Winter Conference on Applications of Computer Vision*, pages 837–847, 2023.

[26] Xiao Jiang, Fei Zhou, and Jiongzhi Lin. Adv2e: Bridging the gap between analogue circuit and discrete frames in the video-to-events simulator, 2024.

[27] Damien Joubert, Alexandre Marcireau, Nic Ralph, Andrew Jolley, André Van Schaik, and Gregory Cohen. Event camera simulator improvements via characterized parameters. *Frontiers in Neuroscience*, 15:702765, 2021.

[28] Damien Joubert, Alexandre Marcireau, Nic Ralph, Andrew Jolley, André van Schaik, and Gregory Cohen. Event camera simulator improvements via characterized parameters. *Frontiers in Neuroscience*, 15:702765, 2021.

[29] Jacques Kaiser, Juan Camilo Vasquez Tieck, Christian Hubschneider, Peter Wolf, Michael Weber, Michael Hoff, Alexander Friedrich, Konrad Wojtasik, Arne Rönnau, Ralf Kohlhaas, Rüdiger Dillmann, and Johann Marius Zöllner. Towards a framework for end-to-end control of a simulated vehicle with spiking neural networks. *2016 IEEE International Conference on Simulation, Modeling, and Programming for Autonomous Robots (SIMPAR)*, pages 127–134, 2016.

[30] Junjie Ke, Qifei Wang, Yilin Wang, Peyman Milanfar, and Feng Yang. Musiq: Multi-scale image quality transformer. In *Proceedings of the IEEE/CVF international conference on computer vision*, pages 5148–5157, 2021.

[31] Bernhard Kerbl, Georgios Kopanas, Thomas Leimkühler, and George Drettakis. 3d gaussian splatting for real-time radiance field rendering. *ACM Transactions on Graphics (TOG)*, 2023.

[32] Simon Klenk, Lukas Koestler, Davide Scaramuzza, and Daniel Cremers. E-nerf: Neural radiance fields from a moving event camera. *IEEE Robotics and Automation Letters*, 8(3):1587–1594, 2023.

[33] Seungjun Lee and Gim Hee Lee. Diet-gs: Diffusion prior and event stream-assisted motion deblurring 3d gaussian splatting, 2025.

[34] Hao Li, He Cao, Bin Feng, Yanjun Shao, Xiangru Tang, Zhiyuan Yan, Li Yuan, Yonghong Tian, and Yu Li. Beyond chemical qa: Evaluating llm's chemical reasoning with modular chemical operations. *arXiv preprint arXiv:2505.21318*, 2025.

[35] Wenpu Li, Pian Wan, Peng Wang, Jinghang Li, Yi Zhou, and Peidong Liu. Benerf: neural radiance fields from a single blurry image and event stream. In *European Conference on Computer Vision*, pages 416–434. Springer, 2025.

[36] Bohao Liao, Wei Zhai, Zengyu Wan, Tianzhu Zhang, Yang Cao, and Zheng-Jun Zha. Ef-3dgs: Event-aided free-trajectory 3d gaussian splatting. *arXiv preprint arXiv:2410.15392*, 2024.

[37] Songnan Lin, Ye Ma, Zhenhua Guo, and Bihan Wen. Dvs-voltmeter: Stochastic process-based event simulator for dynamic vision sensors. In *European Conference on Computer Vision (ECCV)*, 2022.

[38] Lu Ling, Yichen Sheng, Zhi Tu, Wentian Zhao, Cheng Xin, Kun Wan, Lantao Yu, Qianyu Guo, Zixun Yu, Yawen Lu, et al. Dl3dv-10k: A large-scale scene dataset for deep learning-based 3d vision. In *Proceedings of the IEEE/CVF Conference on Computer Vision and Pattern Recognition*, pages 22160–22169, 2024.

[39] Peidong Liu, Xingxing Zuo, Viktor Larsson, and Marc Pollefeys. MBA-VO: Motion Blur Aware Visual Odometry. In *International Conference on Computer Vision (ICCV)*, 2021.

[40] Xialei Liu, Joost Van De Weijer, and Andrew D Bagdanov. Rankiqa: Learning from rankings for no-reference image quality assessment. In *Proceedings of the IEEE international conference on computer vision*, pages 1040–1049, 2017.

[41] Weng Fei Low and Gim Hee Lee. Robust e-nerf: Nerf from sparse & noisy events under non-uniform motion. In *Proceedings of the IEEE/CVF International Conference on Computer Vision*, 2023.

[42] Weng Fei Low and Gim Hee Lee. Deblur e-nerf: Nerf from motion-blurred events under high-speed or low-light conditions. In *European Conference on Computer Vision*, pages 192–209. Springer, 2025.

[43] Qi Ma, Danda Pani Paudel, Ajad Chhatkuli, and Luc Van Gool. Deformable neural radiance fields using rgb and event cameras. In *Proceedings of the IEEE/CVF International Conference on Computer Vision*, pages 3590–3600, 2023.

[44] Yongrui Ma, Shi Guo, Yutian Chen, Tianfan Xue, and Jinwei Gu. Timelens-xl: Real-time event-based video frame interpolation with large motion. In *European Conference on Computer Vision*, pages 178–194. Springer, 2024.

[45] Elias Mueggler, Henri Rebecq, Guillermo Gallego, Tobi Delbruck, and Davide Scaramuzza. The event-camera dataset and simulator: Event-based data for pose estimation, visual odometry, and slam. *International Journal of Robotics Research*, 36(2):142–149, 2017.

[46] Elias Mueggler, Henri Rebecq, Guillermo Gallego, Tobi Delbruck, and Davide Scaramuzza. The event-camera dataset and simulator: Event-based data for pose estimation, visual odometry, and slam. *The International Journal of Robotics Research*, 36(2):142–149, 2017.

[47] Liyuan Pan, Miaomiao Liu, and Richard Hartley. Single image optical flow estimation with an event camera. In *Computer Vision and Pattern Recognition (CVPR)*, 2020.

[48] Md Jubaer Hossain Pantho, Joel Mandebi Mbongue, Pankaj Bhowmik, and Christophe Bobda. Event camera simulator design for modeling attention-based inference architectures. *Journal of Real-Time Image Processing*, 19(2):363–374, 2022.

[49] Cheng Peng, Yutao Tang, Yifan Zhou, Nengyu Wang, Xijun Liu, Deming Li, and Rama Chellappa. Bags: Blur agnostic gaussian splatting through multi-scale kernel modeling. In *European Conference on Computer Vision*, pages 293–310. Springer, 2024.

[50] Mirco Planamente, Chiara Plizzari, Marco Cannici, Marco Ciccone, Francesco Strada, Andrea Bottino, Matteo Matteucci, and Barbara Caputo. Da4event: towards bridging the sim-to-real gap for event cameras using domain adaptation. *IEEE Robotics and Automation Letters*, 6(4):6616–6623, 2021.

[51] Mirco Planamente, Chiara Plizzari, Marco Cannici, Marco Ciccone, Francesco Strada, Andrea Bottino, Matteo Matteucci, and Barbara Caputo. Da4event: towards bridging the sim-to-real gap for event cameras using domain adaptation. *IEEE Robotics and Automation Letters*, 6(4):6616–6623, 2021.

[52] Yunshan Qi, Lin Zhu, Yu Zhang, and Jia Li. E2nerf: Event enhanced neural radiance fields from blurry images. In *International Conference on Computer Vision (ICCV)*, 2023.

[53] Yunshan Qi, Lin Zhu, Yifan Zhao, Nan Bao, and Jia Li. Deblurring neural radiance fields with event-driven bundle adjustment. In *Proceedings of the 32nd ACM International Conference on Multimedia*, pages 9262–9270, 2024.

[54] Henri Rebecq, Daniel Gehrig, and Davide Scaramuzza. Esim: an open event camera simulator. In *Conference on robot learning*, pages 969–982. PMLR, 2018.

[55] Henri Rebecq, René Ranftl, Vladlen Koltun, and Davide Scaramuzza. High speed and high dynamic range video with an event camera. *IEEE Trans. Pattern Anal. Mach. Intell. (T-PAMI)*, 2019.

[56] Antoni Rosinol, John J Leonard, and Luca Carlone. Nerf-slam: Real-time dense monocular slam with neural radiance fields. In *International Conference on Intelligent Robots and Systems (IROS)*, 2023.

[57] Viktor Rudnev, Mohamed Elgharib, Christian Theobalt, and Vladislav Golyanik. Eventnerf: Neural radiance fields from a single colour event camera. In *Computer Vision and Pattern Recognition (CVPR)*, 2023.

[58] Viktor Rudnev, Gereon Fox, Mohamed Elgharib, Christian Theobalt, and Vladislav Golyanik. Dynamic eventnerf: Reconstructing general dynamic scenes from multi-view event cameras. *arXiv preprint arXiv:2412.06770*, 2024.

[59] Johannes L Schonberger and Jan-Michael Frahm. Structure-from-motion Revisited. In *Computer Vision and Pattern Recognition (CVPR)*, 2016.

[60] Wei Shang, Dongwei Ren, Dongqing Zou, Jimmy S Ren, Ping Luo, and Wangmeng Zuo. Bringing events into video deblurring with non-consecutively blurry frames. In *Proceedings of the IEEE/CVF international conference on computer vision*, pages 4531–4540, 2021.

[61] Timo Stoffregen, Cedric Scheerlinck, Davide Scaramuzza, Tom Drummond, Nick Barnes, Lindsay Kleeman, and Robert Mahony. Reducing the sim-to-real gap for event cameras. In *Computer Vision–ECCV 2020: 16th European Conference, Glasgow, UK, August 23–28, 2020, Proceedings, Part XXVII 16*, pages 534–549. Springer, 2020.

[62] Lei Sun, Christos Sakaridis, Jingyun Liang, Qi Jiang, Kailun Yang, Peng Sun, Yaozu Ye, Kaiwei Wang, and Luc Van Gool. Event-based fusion for motion deblurring with cross-modal attention. In *European Conference on Computer Vision*, pages 412–428. Springer, 2022.

[63] Wei Zhi Tang, Daniel Rebain, Kostantinos G Derpanis, and Kwang Moo Yi. Lse-nerf: Learning sensor modeling errors for deblured neural radiance fields with rgb-event stereo. *arXiv preprint arXiv:2409.06104*, 2024.

[64] Gemma Taverni. *Applications of Silicon Retinas: From Neuroscience to Computer Vision*. PhD thesis, Universität Zürich, 2020.

[65] Stepan Tulyakov, Alfredo Bochicchio, Daniel Gehrig, Stamatios Georgoulis, Yuanyou Li, and Davide Scaramuzza. Time lens++: Event-based frame interpolation with parametric non-linear flow and multi-scale fusion. In *Proceedings of the IEEE/CVF Conference on Computer Vision and Pattern Recognition*, pages 17755–17764, 2022.

[66] Stepan Tulyakov, Daniel Gehrig, Stamatios Georgoulis, Julius Erbach, Mathias Gehrig, Yuanyou Li, and Davide Scaramuzza. Time lens: Event-based video frame interpolation. In *Proceedings of the IEEE/CVF conference on computer vision and pattern recognition*, pages 16155–16164, 2021.

[67] Jianyi Wang, Kelvin CK Chan, and Chen Change Loy. Exploring clip for assessing the look and feel of images. In *AAAI*, 2023.

[68] Jiaxu Wang, Junhao He, Ziyi Zhang, Mingyuan Sun, Jingkai Sun, and Renjing Xu. Evggs: A collaborative learning framework for event-based generalizable gaussian splatting. *arXiv preprint arXiv:2405.14959*, 2024.

[69] Jiaxu Wang, Junhao He, Ziyi Zhang, and Renjing Xu. Physical priors augmented event-based 3d reconstruction. In *2024 IEEE International Conference on Robotics and Automation (ICRA)*, pages 16810–16817. IEEE, 2024.

[70] Zhou Wang, Alan C Bovik, Hamid R Sheikh, and Eero P Simoncelli. Image quality assessment: from error visibility to structural similarity. *IEEE transactions on image processing*, 13(4):600–612, 2004.

[71] Jay Zhangjie Wu, Yuxuan Zhang, Haithem Turki, Xuanchi Ren, Jun Gao, Mike Zheng Shou, Sanja Fidler, Zan Gojcic, and Huan Ling. Difix3d+: Improving 3d reconstructions with single-step diffusion models, 2025.

[72] Jingqian Wu, Shuo Zhu, Chutian Wang, Boxin Shi, and Edmund Y Lam. Sweepevgs: Event-based 3d gaussian splatting for macro and micro radiance field rendering from a single sweep. *arXiv preprint arXiv:2412.11579*, 2024.

[73] Tianyi Xiong, Jiayi Wu, Botao He, Cornelia Fermuller, Yiannis Aloimonos, Heng Huang, and Christopher A Metzler. Event3dgs: Event-based 3d gaussian splatting for fast egomotion. *arXiv preprint arXiv:2406.02972*, 2024.

[74] Chuanzhi Xu, Haoxian Zhou, Haodong Chen, Vera Chung, and Qiang Qu. A survey on event-driven 3d reconstruction: Development under different categories. *arXiv preprint arXiv:2503.19753*, 2025.

[75] Chuanzhi Xu, Haoxian Zhou, Haodong Chen, Vera Chung, and Qiang Qu. A survey on event-driven 3d reconstruction: Development under different categories. *arXiv preprint arXiv:2503.19753*, 2025.

[76] Chuanzhi Xu, Haoxian Zhou, Langyi Chen, Haodong Chen, Ying Zhou, Vera Chung, and Qiang Qu. A survey of 3d reconstruction with event cameras: From event-based geometry to neural 3d rendering, 2025.

[77] Wenhao Xu, Wenming Weng, Yueyi Zhang, Ruikang Xu, and Zhiwei Xiong. Event-boosted deformable 3d gaussians for fast dynamic scene reconstruction. *arXiv preprint arXiv:2411.16180*, 2024.

[78] Xiaoting Yin, Hao Shi, Yuhan Bao, Zhenshan Bing, Yiyi Liao, Kailun Yang, and Kaiwei Wang. E-3dgs: Gaussian splatting with exposure and motion events. *arXiv preprint arXiv:2410.16995*, 2024.

[79] Wangbo Yu, Chaoran Feng, Jiye Tang, Xu Jia, Li Yuan, and Yonghong Tian. Evagaussians: Event stream assisted gaussian splatting from blurry images. *arXiv preprint arXiv:2405.20224*, 2024.

[80] Xianggang Yu, Mutian Xu, Yidan Zhang, Haolin Liu, Chongjie Ye, Yushuang Wu, Zizheng Yan, Chenming Zhu, Zhangyang Xiong, Tianyou Liang, et al. Mvimgnet: A large-scale dataset of multi-view images. In *Proceedings of the IEEE/CVF conference on computer vision and pattern recognition*, pages 9150–9161, 2023.

[81] Toshiya Yura, Ashkan Mirzaei, and Igor Gilitschenski. Eventsplat: 3d gaussian splatting from moving event cameras for real-time rendering. *arXiv preprint arXiv:2412.07293*, 2024.

[82] Sohaib Zahid, Viktor Rudnev, Eddy Ilg, and Vladislav Golyanik. E-3dgs: Event-based novel view rendering of large-scale scenes using 3d gaussian splatting. *3DV*, 2025.

[83] Richard Zhang, Phillip Isola, Alexei A Efros, Eli Shechtman, and Oliver Wang. The unreasonable effectiveness of deep features as a perceptual metric. In *Proceedings of the IEEE conference on computer vision and pattern recognition*, pages 586–595, 2018.

[84] Zhongyang Zhang, Shuyang Cui, Kaidong Chai, Haowen Yu, Subhasis Dasgupta, Upal Mahbub, and Tauhidur Rahman. V2CE: Video to continuous events simulator. In *IEEE International Conference on Robotics and Automation (ICRA)*, 2024.

[85] Ziran Zhang, Xiaohui Li, Yihao Liu, Yujin Wang, Yueting Chen, Tianfan Xue, and Shi Guo. Egvd: Event-guided video diffusion model for physically realistic large-motion frame interpolation. *arXiv preprint arXiv:2503.20268*, 2025.

[86] Zixin Zhang, Kanghao Chen, and Lin Wang. Elite-evgs: Learning event-based 3d gaussian splatting by distilling event-to-video priors. *arXiv preprint arXiv:2409.13392*, 2024.

[87] Lingzhe Zhao, Peng Wang, and Peidong Liu. Bad-gaussians: Bundle adjusted deblur gaussian splatting. *arXiv preprint arXiv:2403.11831*, 2024.

[88] Alex Zihao Zhu, Dinesh Thakur, Tolga Özaslan, Bernd Pfrommer, Vijay Kumar, and Kostas Daniilidis. The multivehicle stereo event camera dataset: An event camera dataset for 3d perception. *IEEE Robotics and Automation Letters*, 3(3):2032–2039, 2018.

[89] Alex Zihao Zhu, Ziyun Wang, Kaung Khant, and Kostas Daniilidis. Eventgan: Leveraging large scale image datasets for event cameras. pages 1–11, 2021.

[90] Alex Zihao Zhu, Liangzhe Yuan, Kenneth Chaney, and Kostas Daniilidis. Unsupervised event-based learning of optical flow, depth, and egomotion. In *Computer Vision and Pattern Recognition (CVPR)*, 2019.

A Details of Velocity-Controlled Reparameterization

In our code, we provide two ways to precisely control speed. These are using continuously defined functions and a discrete speed list.

A.1 Continuous speed function

A positive, analytic function

$$v : [0, 1] \to \mathbb{R}_{>0} \quad \text{(dimensionless)},$$

sampled at normalised time t, directly prescribes the speed curve. In the released dataset we adopt

$$v(t) = 0.25 \, \sin(t) + 1.1, \quad t \in [0, 1], \tag{13}$$

A.2 Speed list

An arbitrary-length float array $\mathbf{r} = \{r_k\}_{k=0}^{L-1}$ ($r_k > 0$) is interpreted as *multipliers* of a base frame rate $f_{\text{base}} = 2400$ fps: the k-th temporal segment $\left[t_k, t_{k+1}\right]$ of length $\Delta T = T/L$ is rendered at $f_k = r_k f_{\text{base}}$. To obtain a *continuous* speed curve we blend neighbouring segments with a cubic B-spline[1] in a 2τ-second window centred at each boundary,

$$v(t) = \text{Bspline}\big(t;\, \mathbf{r}, \tau\big), \qquad \tau \simeq 0.1 \, \Delta T.$$

A.3 From speed curve to arc-length samples

Let M be the desired number of interpolated frames, we sample the chosen speed interface on a uniform grid $t_j = j/(M-1)$:

$$u_j = v(t_j), \quad j = 0, \ldots, M-2; \tag{14}$$

$$\Delta s_j = \frac{u_j}{\sum_{k=0}^{M-2} u_k} \, S; \tag{15}$$

$$s_0 = 0, \quad s_{j+1} = s_j + \Delta s_j. \tag{16}$$

Equation (15) rescales the sampled speeds so that $\sum_j \Delta s_j = S$, ensuring the full geometric path is covered.

A.4 Evaluating the spline

Each interpolated pose $\tilde{P}_j = (\tilde{R}_j, \tilde{\mathbf{T}}_j)$ is obtained by querying the spline at the renormalised arc-length $s_j^\star$:

$$\tilde{P}_j = \mathcal{P}\big(s_j\big), \qquad j = 0, \ldots, M-1.$$

Because $s_{j+1} - s_j \propto v(t_j)$, the linear and angular velocities of the discrete trajectory $\{\tilde{P}_j\}$ follow the prescribed speed profile with frame-level accuracy.

A.5 Practical remarks

- **Choice of interface.** The analytic form (13) is convenient for dataset-level consistency; the speed list form offers frame-accurate speed control for bespoke sequences.
- **Continuity.** Both interfaces yield a C^2 speed curve, hence the final trajectory is at least C^1, avoiding jerk during rendering.
- **Complexity.** The whole pipeline is linear in $N+M$ and is CPU-friendly ($< 0.5\,\mu$s per interpolated pose).

Summary. Either a compact analytic law (13) or an arbitrary-length speed list can be mapped, via Eq. (15), to B-spline arc-length samples, providing reliable and precise control over camera velocity for every rendered frame.

[1] Order 3 suffices to reach C^2 continuity while keeping local support.

B Details of choosing the contrast threshold

In our experiments, we found that when we set the contrast threshold $c \leq 0.75$, visible floater artifacts appeared during the visualization of the event stream. These artifacts occur when the viewpoint changes and certain Gaussians—originally situated in the background and expected to be occluded—are mistakenly treated as part of the visible foreground. This misclassification leads to variations in illumination that induce apparent voltage changes, which the simulator erroneously interprets as valid event triggers. As a result, the synthesized event stream contains non-physical textures, manifesting as spurious structures or noise in the visualization. As shown in the figure 7, once we raise c to 1 or higher, the floater becomes almost invisible.

It is worth noting that when the contrast threshold is set too low, according to the research results in [51], it will lead to a loss of dynamic range. Therefore, in this paper, we tend to set a larger c to solve both problems simultaneously. To ensure that events are not overly sparse and sufficient information integrity is retained, the GS2E dataset was simulated with the parameter setting $c = 1$.

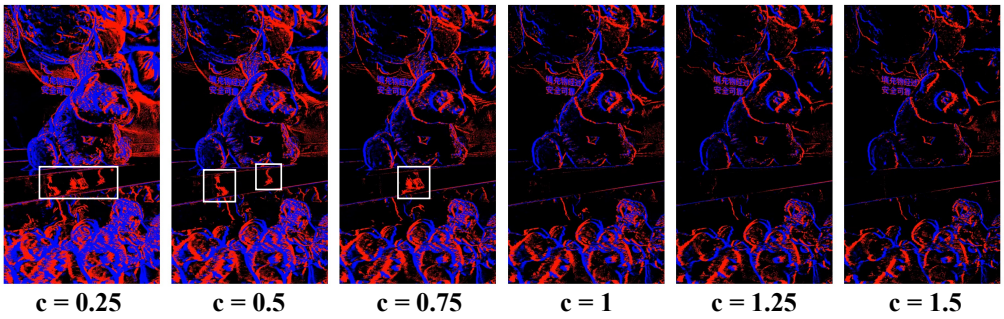

Figure 7: Selecting the same viewpoint and time window(1000 us), visualize events simulated from 3DGS with different contrast threshold(c) values. The results show that when $c \leq 0.75$, error events generated by floater Gaussians can be seen on the integral event diagram, while this phenomenon is greatly alleviated when $c \geq 1$.

C Implementation Details

For the reconstruction stage, we carefully collect approximately 2k high-quality multi-view images from 2 public datasets: MVImageNet [80] and DL3DV [38]: we choose and render 1.8k scenes from MVImageNet and 100 scenes from DL3DV. We employ the official interplementation verision of 3DGS [31] in the original setting. For the event generation stage, we utilize the DVS-Voltmeter simulator [37] to synthesize events from the rendered RGB sequences. We adopt the following sensor-specific parameters to closely mimic the behavior of real DVS sensors: the ON and OFF contrast thresholds are both set to $\Theta_{\text{ON}} = \Theta_{\text{OFF}} = 1$ as default. The dvs camera parameters are calibrated as $k_1 = 0.5, k_2 = 1e-3, k_3 = 0.1, k_4 = 0.01, k_5 = 0.1, k_6 = 1e-5$, following the original DVS-Voltmeter setting. These control the brightness-dependent drift μ and variance σ^2 of the stochastic process, which determine the polarity distribution and the inverse-Gaussian timestamp sampling for each event.

All events are simulated at 2400 FPS temporal resolution and stored with microsecond timestamps for high-fidelity spatio-temporal alignment. The overall process are conducted on a workstation equipped with 8×NVIDIA RTX 3090 GPUs. The selected MVImageNet clip images vary in size, but most are approximately 1080p in resolution. When training 3DGS on MVImageNet, each scene takes an average of 16 minutes. For the camera pose upsampling and trajectory control stage, using an interpolation factor of $\gamma = 5$, the strategy `ada_speed`, and the velocity function $v(t) = 0.25\sin(t) + 1.1$, the average runtime per scene is approximately 45 seconds.

During event simulation, we adopt the same camera parameter configuration as mentioned previously. However, the simulation time varies significantly depending on the motion amplitude and speed of the camera, as well as the scene complexity, making it difficult to estimate a consistent runtime.

For the DL3DV dataset, each scene contains 300–400 images. To ensure higher reconstruction and rendering quality, as well as to generate longer event streams, we do not downsample the input image

resolution, nor do we slice the image or event sequences. Using the same hardware configuration as with MVImageNet, the average per-scene training time is approximately 27 minutes, and the rendering time is around 41 minutes.

D Existing Event-based 3D Reconstruction Datasets

To contextualize the contribution of GS2E, Table 5 provides a comprehensive comparison of existing event-based 3D datasets and 3D reconstruction methods [43, 9, 52, 2, 82, 63, 87, 53, 58, 79, 89, 73, 77, 24, 18, 57, 72, 1, 78, 81, 41, 42, 86, 68, 25, 88, 39, 15, 35, 49, 4, 22, 66, 17, 11, 85, 44, 21]. We categorize these into **static scenes** and **dynamic scenes**, based on whether the underlying geometry remains constant or involves temporal variation.

Attributes. Each dataset is evaluated along key axes:

- **Data Type:** Whether sharp and/or blurry RGB frames are provided. Blurry frames support deblurring tasks, while sharp ones aid in geometry fidelity.
- **Scene Num / Scale:** Number of distinct scenes and their spatial scope (object-level vs. medium/large indoor scenes).
- **GT Poses:** Availability of ground-truth camera extrinsics.
- **Speed Profile:** Whether camera motion follows uniform or non-uniform velocity.
- **Multi-Trajectory:** Whether each scene supports multiple trajectory simulations, enabling consistent multi-view observations.
- **Device:** Capture source—real event sensors (e.g., DAVIS346C, DVXplore) or simulated streams (e.g., ESIM, Vid2E, V2E).
- **Data Source:** Origin of the base scene data (e.g., NeRF renderings, Blender, Unreal Engine, or real-world scenes).

Key Findings. We observe that existing datasets are limited in several aspects:

- Most datasets focus on small-scale, object-centric scenes with limited spatial or temporal diversity.
- Simulators typically use simplified trajectories and fixed contrast thresholds, which constrain realism.
- Real event data remains scarce and often lacks consistent trajectory coverage or paired ground truth.
- Multi-trajectory support is rare, impeding evaluation under view-consistency and generalization settings.

Positioning of GS2E. Our proposed GS2E benchmark is designed to address these limitations by:

- Leveraging 3D Gaussian Splatting to reconstruct photorealistic static scenes from sparse real-world RGB inputs.
- Generating controllable, dense virtual trajectories with adaptive speed profiles and multiple interpolated paths per scene.
- Synthesizing events via a physically-informed simulator that incorporates realistic contrast threshold modeling.
- Supporting both object- and scene-level scales with consistent multi-view alignment and temporal density.

By filling the gaps in scale, realism, and trajectory diversity, GS2E enables more robust evaluation of event-based 3D reconstruction and rendering methods.

E Limitation and Broader impacts

Limitation. While GS2E provides high-fidelity, geometry-consistent event data under a wide range of camera trajectories and motion patterns, it remains fundamentally limited by its reliance on rendered RGB images from 3DGS. Specifically, the current pipeline inherits the photometric constraints of 3D Gaussian Splatting , which may not faithfully replicate extreme illumination conditions such as overexposure or underexposure. As a result, scenes with very low light or high dynamic range may not be accurately modeled in terms of event triggering behavior. Additionally, our framework currently assumes static scenes; dynamic object motion is not yet modeled. In future work, we plan to extend the simulator by incorporating physically-realistic camera models into the 3DGS rendering pipeline, enabling explicit control over exposure, tone mapping, and sensor response curves to better approximate real-world lighting variability.

Broader impacts. This work introduces a scalable, geometry-consistent synthetic dataset for event-based vision research. On the positive side, it lowers the barrier for training high-performance models in domains such as autonomous driving, robotics, and augmented reality, where event-based sensing offers advantages under fast motion or challenging lighting. By providing a flexible, physically-grounded simulation framework, the work supports reproducible and ethical AI development. On the negative side, improved realism in synthetic event data may inadvertently enable misuse such as generating adversarial inputs or synthetic surveillance data. These risks are mitigated by the dataset's academic licensing and transparency in its construction pipeline. Furthermore, the data generation framework may raise privacy concerns if adapted for real-scene reproduction, which warrants further community discussion and the adoption of usage safeguards.

F License of the used assets

- **3D Gaussian Splatting [31]**: A publicly available method with its dataset released under the CC BY MIT license.
- **MVImgNet [80]**: A publicly available dataset released under the CC BY 4.0 license.
- **DL3DV [38]**: A publicly available dataset released under the CC BY 4.0 license.
- **GS2E**: A publicly available dataset released under the CC BY MIT license.

Method	Column	Type	Color Frame		Scene Num	Scene Scale	GT poses	Speed	Multi-Trajectory	Device	Data Source
			Blurry	Sharp							
Static Scenes											
Event-NeRF [57]	CVPR 2023	Synthetic	×	✓	7	object	✓	Uniform	×	Blender+ESIM	NeRF
E2NeRF [52]	ICCV 2023	Synthetic	✓	✓	7	object	✓	Uniform	×	Blender+ESIM	NeRF
		Real	✓	×	5	medium&large	×	Uniform	×	DAVIS346C	Author Collection
Robust e-NeRF [41]	ICCV 2023	Synthetic	×	✓	7	object	✓	Non-Uniform	✓	Blender+ESIM	NeRF
Deblur e-NeRF [42]	ECCV 2024	Synthetic	×	✓	7	object	✓	Non-Uniform	✓	Blender+ESIM	NeRF
EvaGaussian [79]	Arxiv 2024	Synthetic	✓	✓	9	medium&large	✓	Uniform	✓	Blender+ESIM	NeRF, Deblur-NeRF +Author Collection
		Real	✓	×	5	medium&large	×	Uniform	×	DAVIS346C	Author Collection
PAEv3D [69]	ICRA 2024	Real	×	✓	6	object	×	Uniform	×	DVXplore event camera	Author Collection
EvDebluRF	CVPR 2024	Synthetic	✓	✓	4	medium	✓	Uniform	×	Blender+ESIM	Deblur-NeRF
		Real	✓	×	5	medium	×	Uniform	×	DAVIS346C	Author Collection
EvGGS [68]	ICML 2024	Synthetic	×	×	64	object	✓	Uniform	×	Blender+V2E	Author Collection
IncEventGS [24]	CVPR 2025	Synthetic	×	✓	6	large	✓	Uniform	×	Vid2E	Replica
E-3DGS [82]	3DV 2025	Synthetic	×	✓	3	medium	✓	Non-Uniform	×	-	UnrealEgo
AE-NeRF [9]	AAAI 2025	Synthetic	×	✓	3	medium	✓	Non-Uniform	×	-	UnrealEgo
EF-3DGS [36]	Arxiv 2024	Synthetic	×	✓	9	large	✓	Uniform	×	Vid2E	Tanks and Temples
LSE-NeRF [63]	Arxiv 2024	Real	✓	✓	10	medium&large	✓	Non-Uniform	-	Prophesee EVK-3 HD + Blackfly S (GigE)	Author Collection
GS2E	**Submission**	**Synthetic**	✓	✓	**1150**	**medium&large**	✓	**Non-Uniform**	✓	**3DGS + DVS-Voltmetre**	**Author Collection**
Dynamic Scenes											
DE-NeRF [43]	ICCV 2023	Synthetic	×	✓	3	object	✓	Uniform	×	Blender+ESIM	Author Collection
		Real	×	✓	6	medium&large	✓	Uniform	×	Samsung DVS Gen3, DAVIS 346C	Color Event Camera, HS-ERGB(Timeslen)
EvDNeRF [1]	CVPR 2024 Workshop	Synthetic	×	×	3	object	✓	Uniform	✓	Blender+ESIM	Kubric
Dynamic EventNeRF [58]	CVPR 2025 Workshop	Synthetic	×	✓	5	object	✓	Uniform	✓	Blender+ESIM	Author Collection
		Real	×	✓	16	medium&large	✓	Uniform	✓	DAVIS346C	Author Collection

Table 5: Comparison of existing event-based 3D reconstruction datasets, categorized by scene type, motion profile, sensor modality, and simulation pipeline.

NeurIPS Paper Checklist

The checklist is designed to encourage best practices for responsible machine learning research, addressing issues of reproducibility, transparency, research ethics, and societal impact. Do not remove the checklist: **The papers not including the checklist will be desk rejected.** The checklist should follow the references and follow the (optional) supplemental material. The checklist does NOT count towards the page limit.

Please read the checklist guidelines carefully for information on how to answer these questions. For each question in the checklist:

- You should answer [Yes] , [No] , or [NA] .
- [NA] means either that the question is Not Applicable for that particular paper or the relevant information is Not Available.
- Please provide a short (1–2 sentence) justification right after your answer (even for NA).

The checklist answers are an integral part of your paper submission. They are visible to the reviewers, area chairs, senior area chairs, and ethics reviewers. You will be asked to also include it (after eventual revisions) with the final version of your paper, and its final version will be published with the paper.

The reviewers of your paper will be asked to use the checklist as one of the factors in their evaluation. While "[Yes] " is generally preferable to "[No] ", it is perfectly acceptable to answer "[No] " provided a proper justification is given (e.g., "error bars are not reported because it would be too computationally expensive" or "we were unable to find the license for the dataset we used"). In general, answering "[No] " or "[NA] " is not grounds for rejection. While the questions are phrased in a binary way, we acknowledge that the true answer is often more nuanced, so please just use your best judgment and write a justification to elaborate. All supporting evidence can appear either in the main paper or the supplemental material, provided in appendix. If you answer [Yes] to a question, in the justification please point to the section(s) where related material for the question can be found.

IMPORTANT, please:

- **Delete this instruction block, but keep the section heading "NeurIPS Paper Checklist"**,
- **Keep the checklist subsection headings, questions/answers and guidelines below.**
- **Do not modify the questions and only use the provided macros for your answers**.

1. **Claims**

   Question: Do the main claims made in the abstract and introduction accurately reflect the paper's contributions and scope?

   Answer: [Yes]

   Justification: We analyzed the limitations of existing event-based datasets and proposed a novel dataset using 3D rendering techniques to address these limitations. We experimentally demonstrated that the proposed dataset can compensate for the weaknesses of existing datasets in terms of generalizability.

   Guidelines:

   - The answer NA means that the abstract and introduction do not include the claims made in the paper.
   - The abstract and/or introduction should clearly state the claims made, including the contributions made in the paper and important assumptions and limitations. A No or NA answer to this question will not be perceived well by the reviewers.
   - The claims made should match theoretical and experimental results, and reflect how much the results can be expected to generalize to other settings.
   - It is fine to include aspirational goals as motivation as long as it is clear that these goals are not attained by the paper.

2. **Limitations**

   Question: Does the paper discuss the limitations of the work performed by the authors?

Answer: [Yes]

Justification: See Appendix E.

Guidelines:

- The answer NA means that the paper has no limitation while the answer No means that the paper has limitations, but those are not discussed in the paper.
- The authors are encouraged to create a separate "Limitations" section in their paper.
- The paper should point out any strong assumptions and how robust the results are to violations of these assumptions (e.g., independence assumptions, noiseless settings, model well-specification, asymptotic approximations only holding locally). The authors should reflect on how these assumptions might be violated in practice and what the implications would be.
- The authors should reflect on the scope of the claims made, e.g., if the approach was only tested on a few datasets or with a few runs. In general, empirical results often depend on implicit assumptions, which should be articulated.
- The authors should reflect on the factors that influence the performance of the approach. For example, a facial recognition algorithm may perform poorly when image resolution is low or images are taken in low lighting. Or a speech-to-text system might not be used reliably to provide closed captions for online lectures because it fails to handle technical jargon.
- The authors should discuss the computational efficiency of the proposed algorithms and how they scale with dataset size.
- If applicable, the authors should discuss possible limitations of their approach to address problems of privacy and fairness.
- While the authors might fear that complete honesty about limitations might be used by reviewers as grounds for rejection, a worse outcome might be that reviewers discover limitations that aren't acknowledged in the paper. The authors should use their best judgment and recognize that individual actions in favor of transparency play an important role in developing norms that preserve the integrity of the community. Reviewers will be specifically instructed to not penalize honesty concerning limitations.

3. **Theory assumptions and proofs**

   Question: For each theoretical result, does the paper provide the full set of assumptions and a complete (and correct) proof?

   Answer: [NA]

   Justification:

   Guidelines:

   - The answer NA means that the paper does not include theoretical results.
   - All the theorems, formulas, and proofs in the paper should be numbered and cross-referenced.
   - All assumptions should be clearly stated or referenced in the statement of any theorems.
   - The proofs can either appear in the main paper or the supplemental material, but if they appear in the supplemental material, the authors are encouraged to provide a short proof sketch to provide intuition.
   - Inversely, any informal proof provided in the core of the paper should be complemented by formal proofs provided in appendix or supplemental material.
   - Theorems and Lemmas that the proof relies upon should be properly referenced.

4. **Experimental result reproducibility**

   Question: Does the paper fully disclose all the information needed to reproduce the main experimental results of the paper to the extent that it affects the main claims and/or conclusions of the paper (regardless of whether the code and data are provided or not)?

   Answer: [Yes]

   Justification: In Section 3, we described the 3D volume rendering based on 3DGS, event generation model, and data and trajectory augmentation we used, and specify the hyperparameters to reproduce the proposed pipeline. We also specify the configuration for training the deep networks used in our experiments.

Guidelines:

- The answer NA means that the paper does not include experiments.
- If the paper includes experiments, a No answer to this question will not be perceived well by the reviewers: Making the paper reproducible is important, regardless of whether the code and data are provided or not.
- If the contribution is a dataset and/or model, the authors should describe the steps taken to make their results reproducible or verifiable.
- Depending on the contribution, reproducibility can be accomplished in various ways. For example, if the contribution is a novel architecture, describing the architecture fully might suffice, or if the contribution is a specific model and empirical evaluation, it may be necessary to either make it possible for others to replicate the model with the same dataset, or provide access to the model. In general. releasing code and data is often one good way to accomplish this, but reproducibility can also be provided via detailed instructions for how to replicate the results, access to a hosted model (e.g., in the case of a large language model), releasing of a model checkpoint, or other means that are appropriate to the research performed.
- While NeurIPS does not require releasing code, the conference does require all submissions to provide some reasonable avenue for reproducibility, which may depend on the nature of the contribution. For example
  (a) If the contribution is primarily a new algorithm, the paper should make it clear how to reproduce that algorithm.
  (b) If the contribution is primarily a new model architecture, the paper should describe the architecture clearly and fully.
  (c) If the contribution is a new model (e.g., a large language model), then there should either be a way to access this model for reproducing the results or a way to reproduce the model (e.g., with an open-source dataset or instructions for how to construct the dataset).
  (d) We recognize that reproducibility may be tricky in some cases, in which case authors are welcome to describe the particular way they provide for reproducibility. In the case of closed-source models, it may be that access to the model is limited in some way (e.g., to registered users), but it should be possible for other researchers to have some path to reproducing or verifying the results.

5. **Open access to data and code**

   Question: Does the paper provide open access to the data and code, with sufficient instructions to faithfully reproduce the main experimental results, as described in supplemental material?

   Answer: [Yes]

   Justification: We provide nearly 100 scenes for validation and visualization on Hugging Face, along with partial code available on GitHub. Upon acceptance, we will release the full dataset and complete codebase to enable full reproducibility of the data generation process.

   Guidelines:

   - The answer NA means that paper does not include experiments requiring code.
   - Please see the NeurIPS code and data submission guidelines (`https://nips.cc/public/guides/CodeSubmissionPolicy`) for more details.
   - While we encourage the release of code and data, we understand that this might not be possible, so "No" is an acceptable answer. Papers cannot be rejected simply for not including code, unless this is central to the contribution (e.g., for a new open-source benchmark).
   - The instructions should contain the exact command and environment needed to run to reproduce the results. See the NeurIPS code and data submission guidelines (`https://nips.cc/public/guides/CodeSubmissionPolicy`) for more details.
   - The authors should provide instructions on data access and preparation, including how to access the raw data, preprocessed data, intermediate data, and generated data, etc.
   - The authors should provide scripts to reproduce all experimental results for the new proposed method and baselines. If only a subset of experiments are reproducible, they should state which ones are omitted from the script and why.

- At submission time, to preserve anonymity, the authors should release anonymized versions (if applicable).
- Providing as much information as possible in supplemental material (appended to the paper) is recommended, but including URLs to data and code is permitted.

6. **Experimental setting/details**

   Question: Does the paper specify all the training and test details (e.g., data splits, hyperparameters, how they were chosen, type of optimizer, etc.) necessary to understand the results?

   Answer: [Yes]

   Justification: We specified our expermental setting in Section 4 and Appendix C.

   Guidelines:

   - The answer NA means that the paper does not include experiments.
   - The experimental setting should be presented in the core of the paper to a level of detail that is necessary to appreciate the results and make sense of them.
   - The full details can be provided either with the code, in appendix, or as supplemental material.

7. **Experiment statistical significance**

   Question: Does the paper report error bars suitably and correctly defined or other appropriate information about the statistical significance of the experiments?

   Answer: [No]

   Justification:

   Guidelines:

   - The answer NA means that the paper does not include experiments.
   - The authors should answer "Yes" if the results are accompanied by error bars, confidence intervals, or statistical significance tests, at least for the experiments that support the main claims of the paper.
   - The factors of variability that the error bars are capturing should be clearly stated (for example, train/test split, initialization, random drawing of some parameter, or overall run with given experimental conditions).
   - The method for calculating the error bars should be explained (closed form formula, call to a library function, bootstrap, etc.)
   - The assumptions made should be given (e.g., Normally distributed errors).
   - It should be clear whether the error bar is the standard deviation or the standard error of the mean.
   - It is OK to report 1-sigma error bars, but one should state it. The authors should preferably report a 2-sigma error bar than state that they have a 96% CI, if the hypothesis of Normality of errors is not verified.
   - For asymmetric distributions, the authors should be careful not to show in tables or figures symmetric error bars that would yield results that are out of range (e.g. negative error rates).
   - If error bars are reported in tables or plots, The authors should explain in the text how they were calculated and reference the corresponding figures or tables in the text.

8. **Experiments compute resources**

   Question: For each experiment, does the paper provide sufficient information on the computer resources (type of compute workers, memory, time of execution) needed to reproduce the experiments?

   Answer: [Yes]

   Justification: We specified our experimental setup in Section 4 and explain our training computation and the cost of the event generation model.

   Guidelines:

   - The answer NA means that the paper does not include experiments.

- The paper should indicate the type of compute workers CPU or GPU, internal cluster, or cloud provider, including relevant memory and storage.
- The paper should provide the amount of compute required for each of the individual experimental runs as well as estimate the total compute.
- The paper should disclose whether the full research project required more compute than the experiments reported in the paper (e.g., preliminary or failed experiments that didn't make it into the paper).

9. **Code of ethics**

   Question: Does the research conducted in the paper conform, in every respect, with the NeurIPS Code of Ethics `https://neurips.cc/public/EthicsGuidelines`?

   Answer: [Yes]

   Justification: We carefully read NeurIPS Code of Ethics and followed the guidelines. We preserve anonymity in all respects.

   Guidelines:

   - The answer NA means that the authors have not reviewed the NeurIPS Code of Ethics.
   - If the authors answer No, they should explain the special circumstances that require a deviation from the Code of Ethics.
   - The authors should make sure to preserve anonymity (e.g., if there is a special consideration due to laws or regulations in their jurisdiction).

10. **Broader impacts**

    Question: Does the paper discuss both potential positive societal impacts and negative societal impacts of the work performed?

    Answer: [Yes]

    Justification: See Appendix D.

    Guidelines:

    - The answer NA means that there is no societal impact of the work performed.
    - If the authors answer NA or No, they should explain why their work has no societal impact or why the paper does not address societal impact.
    - Examples of negative societal impacts include potential malicious or unintended uses (e.g., disinformation, generating fake profiles, surveillance), fairness considerations (e.g., deployment of technologies that could make decisions that unfairly impact specific groups), privacy considerations, and security considerations.
    - The conference expects that many papers will be foundational research and not tied to particular applications, let alone deployments. However, if there is a direct path to any negative applications, the authors should point it out. For example, it is legitimate to point out that an improvement in the quality of generative models could be used to generate deepfakes for disinformation. On the other hand, it is not needed to point out that a generic algorithm for optimizing neural networks could enable people to train models that generate Deepfakes faster.
    - The authors should consider possible harms that could arise when the technology is being used as intended and functioning correctly, harms that could arise when the technology is being used as intended but gives incorrect results, and harms following from (intentional or unintentional) misuse of the technology.
    - If there are negative societal impacts, the authors could also discuss possible mitigation strategies (e.g., gated release of models, providing defenses in addition to attacks, mechanisms for monitoring misuse, mechanisms to monitor how a system learns from feedback over time, improving the efficiency and accessibility of ML).

11. **Safeguards**

    Question: Does the paper describe safeguards that have been put in place for responsible release of data or models that have a high risk for misuse (e.g., pretrained language models, image generators, or scraped datasets)?

    Answer: [NA]

Justification:

Guidelines:

- The answer NA means that the paper poses no such risks.
- Released models that have a high risk for misuse or dual-use should be released with necessary safeguards to allow for controlled use of the model, for example by requiring that users adhere to usage guidelines or restrictions to access the model or implementing safety filters.
- Datasets that have been scraped from the Internet could pose safety risks. The authors should describe how they avoided releasing unsafe images.
- We recognize that providing effective safeguards is challenging, and many papers do not require this, but we encourage authors to take this into account and make a best faith effort.

12. **Licenses for existing assets**

    Question: Are the creators or original owners of assets (e.g., code, data, models), used in the paper, properly credited and are the license and terms of use explicitly mentioned and properly respected?

    Answer: [Yes]

    Justification: See Section F *License of the used assets* in the appendix.

    Guidelines:

    - The answer NA means that the paper does not use existing assets.
    - The authors should cite the original paper that produced the code package or dataset.
    - The authors should state which version of the asset is used and, if possible, include a URL.
    - The name of the license (e.g., CC-BY 4.0) should be included for each asset.
    - For scraped data from a particular source (e.g., website), the copyright and terms of service of that source should be provided.
    - If assets are released, the license, copyright information, and terms of use in the package should be provided. For popular datasets, `paperswithcode.com/datasets` has curated licenses for some datasets. Their licensing guide can help determine the license of a dataset.
    - For existing datasets that are re-packaged, both the original license and the license of the derived asset (if it has changed) should be provided.
    - If this information is not available online, the authors are encouraged to reach out to the asset's creators.

13. **New assets**

    Question: Are new assets introduced in the paper well documented and is the documentation provided alongside the assets?

    Answer:[Yes]

    Justification: Brief documentation for the proposed dataset and generation method are in the dataset card of huggingface website. We will upload the full and completed version upon acceptance.

    Guidelines:

    - The answer NA means that the paper does not release new assets.
    - Researchers should communicate the details of the dataset/code/model as part of their submissions via structured templates. This includes details about training, license, limitations, etc.
    - The paper should discuss whether and how consent was obtained from people whose asset is used.
    - At submission time, remember to anonymize your assets (if applicable). You can either create an anonymized URL or include an anonymized zip file.

14. **Crowdsourcing and research with human subjects**

Question: For crowdsourcing experiments and research with human subjects, does the paper include the full text of instructions given to participants and screenshots, if applicable, as well as details about compensation (if any)?

Answer: [NA]

Justification:

Guidelines:

- The answer NA means that the paper does not involve crowdsourcing nor research with human subjects.
- Including this information in the supplemental material is fine, but if the main contribution of the paper involves human subjects, then as much detail as possible should be included in the main paper.
- According to the NeurIPS Code of Ethics, workers involved in data collection, curation, or other labor should be paid at least the minimum wage in the country of the data collector.

15. **Institutional review board (IRB) approvals or equivalent for research with human subjects**

Question: Does the paper describe potential risks incurred by study participants, whether such risks were disclosed to the subjects, and whether Institutional Review Board (IRB) approvals (or an equivalent approval/review based on the requirements of your country or institution) were obtained?

Answer: [NA]

Justification:

Guidelines:

- The answer NA means that the paper does not involve crowdsourcing nor research with human subjects.
- Depending on the country in which research is conducted, IRB approval (or equivalent) may be required for any human subjects research. If you obtained IRB approval, you should clearly state this in the paper.
- We recognize that the procedures for this may vary significantly between institutions and locations, and we expect authors to adhere to the NeurIPS Code of Ethics and the guidelines for their institution.
- For initial submissions, do not include any information that would break anonymity (if applicable), such as the institution conducting the review.

16. **Declaration of LLM usage**

Question: Does the paper describe the usage of LLMs if it is an important, original, or non-standard component of the core methods in this research? Note that if the LLM is used only for writing, editing, or formatting purposes and does not impact the core methodology, scientific rigorousness, or originality of the research, declaration is not required.

Answer: [NA]

Justification:

Guidelines:

- The answer NA means that the core method development in this research does not involve LLMs as any important, original, or non-standard components.
- Please refer to our LLM policy (`https://neurips.cc/Conferences/2025/LLM`) for what should or should not be described.